

# INVESTIGATING DREDGE PLACEMENT OPTIMISATION TO BENEFIT SURF AMENITY

Nick Naderi <sup>1</sup>, Alexander Atkinson <sup>1</sup>, Kane Nielsen <sup>1</sup>, and Paul Boswood <sup>1</sup>

Dredge material removed from the Tweed River Entrance is deposited offshore from Gold Coast beaches to assist in mitigating erosion. Research was undertaken by the Queensland Government Hydraulics Laboratory (QGHL), in collaboration with Tweed Sand Bypassing (TSB), to investigate the potential of targeting dredge depositions to also improve surf amenity. A time-domain numerical wave model (SWASH) was developed as a design tool and calibrated using physical model data. Overall, SWASH reproduced wave heights over and in the lee of the mound with reasonable accuracy. However, tuning of the breaking parameters ( $\alpha$  and  $\beta$ ) is necessary to accurately simulate the onset and persistence of the breaking process. The results of both physical and numerical modelling highlight the importance of sand mound shape in disrupting the wave field, resulting in breakpoint variability in the mound's lee, which could potentially create more favorable surfing conditions.

*Keywords: SWASH; surf amenity; physical modeling; Tweed Sand Bypassing*

## 1. INTRODUCTION

Foreshore areas of the Gold Coast not only provide significant social and environmental benefits, but also play a crucial role in the tourism and economy of Queensland. The economic value of surfing and beach amenity at the southern Gold Coast and a navigable Tweed River entrance, both for visitors and residents, has been estimated to be approximately \$228 million per year (Raybould and Anning 2020). The Gold Coast was nourished with over 3 million m<sup>3</sup> of sand prior to the Commonwealth Games in 2017 (Colleter et al. 2019). Some of the nourishment's resulting mounds were observed to produce high quality surf waves. Growing demand and interest in surf amenity, and availability of dredge material has inspired the investigation into the potential of targeting dredge depositions to also improve surf amenity.

While Tweed Sand Bypassing (TSB) regularly traps and delivers pumped sand direct to northern beaches, occasional dredge campaigns are still required to maintain the navigability of the Tweed River entrance located on the border between New South Wales and Queensland (Figure 1). Most of the sand removed from the entrance is placed to the north to feed the southern Gold Coast beaches in pre-allocated deposition boxes. The beaches and their nearshore capacities are assessed before the dredging campaign to determine precedence for deposition. For example, any primary deposition locations with receiving capacity are prioritised before determining the remaining volume available for the target mound.

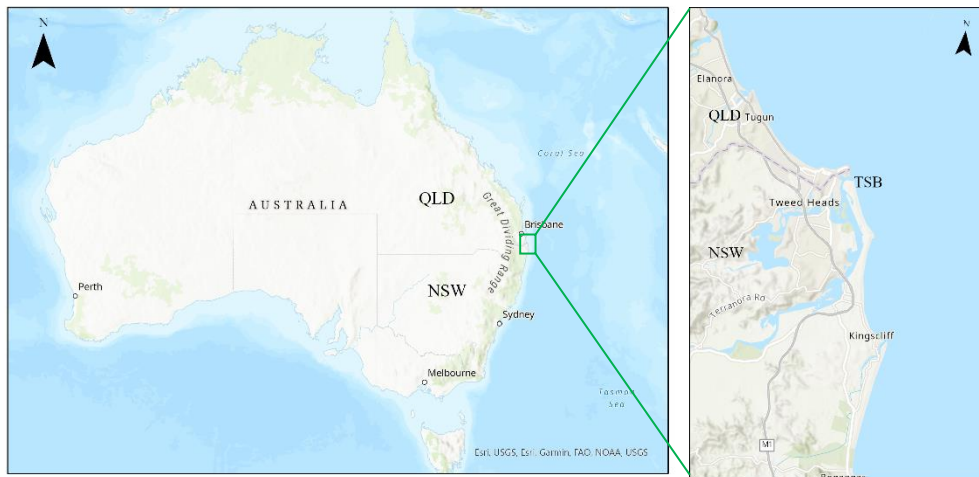


**Figure 1. Location of Tweed Sand Bypassing.**

The key objective of this research is to explore the possibility of using dredge depositions to enhance surf amenity. To assess this potential, a multidisciplinary approach is applied, using physical modelling

<sup>1</sup> Queensland Government Hydraulics Laboratory, 27 Quinlan Street, DEAGON, QLD 4017, Australia.

data in the QGHL wave basin to calibrate and validate a numerical model, SWASH (Simulating WAVes till SHore (Zijlema 2011)), which will be used as a design tool to aid in the future design of placement mound shapes. Future work is intended to collect field data using cameras and pressure transducers to further validate SWASH at the prototype during the upcoming Tweed River Entrance Dredge Campaign and targeted placement (Figure 2). The rest of this paper focuses on physical and numerical modelling. Field data collection and validation of SWASH on the prototype scale will be discussed in a separate paper.

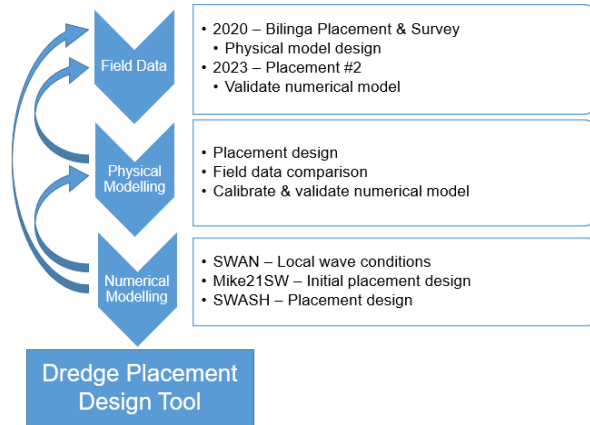


Figure 2. The multidisciplinary approach for preparing a dredge placement design tool.

## 2. Method

To investigate the potential of using dredge depositions to improve surf amenity, a multidisciplinary approach is taken as follows:

- 1- Collecting local wave data using:
  - Available nearby Waverider buoy (Tweed Waverider buoy)
  - Local wave data at the deposition site (Between Bilinga and Tugun)
- 2- Simulating the nearby wave climate
  - Using a nearshore wave model, SWAN (Simulating WAVes Nearshore (Booij 1999))
- 3- Developing a spectral wave model (Mike21SW) to consider initial placement design
- 4- Building a physical model for calibrating the numerical model
- 5- Developing a non-hydrostatic wave-flow model (SWASH) that will initially be calibrated and validated using the physical model.
- 6- Using the validated SWASH model as a design tool for design of placement mound shapes
- 7- Collecting field data for further validation of SWASH at the prototype and comparison with the physical model results.

### 2.1 Local wave climate

Offshore wave buoys and SWAN are used to determine a range of spectral wave conditions to apply to the site. The TSB dredge campaign typically occurs in late Australian winter when required. Therefore, the wave climate for this modelling is determined by consideration of the long-term averages for spring and summer (i.e. September to February) conditions, when the mound should be in place.

#### 2.1.1 Nearby waverider buoys

A decade of offshore wave buoy data from Tweed River wave buoy (location indicated in Figure 3) was used to investigate the range of conditions at the nearest wave rider buoy to the site.

Figure 4 presents the distributions of significant wave height ( $H_s$ ), peak and zero-crossing periods ( $T_p$  and  $T_z$ ) and peak period direction ( $Dir-T_p$ ) for wave directions originating from northerly of 110-degrees (being the southerly-most direct line-of-sight from the placement site to the open ocean). Figure 5 presents a scatter plot of  $H_s$  against  $T_p$  for all the data used to produce the distribution plots in the previous figure.

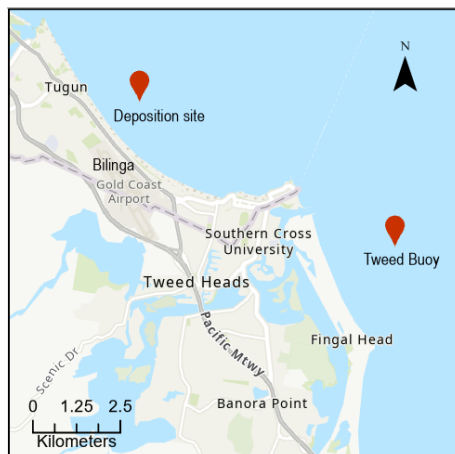


Figure 3. Last recorded location of the Tweed Waverider buoy – deposition site.

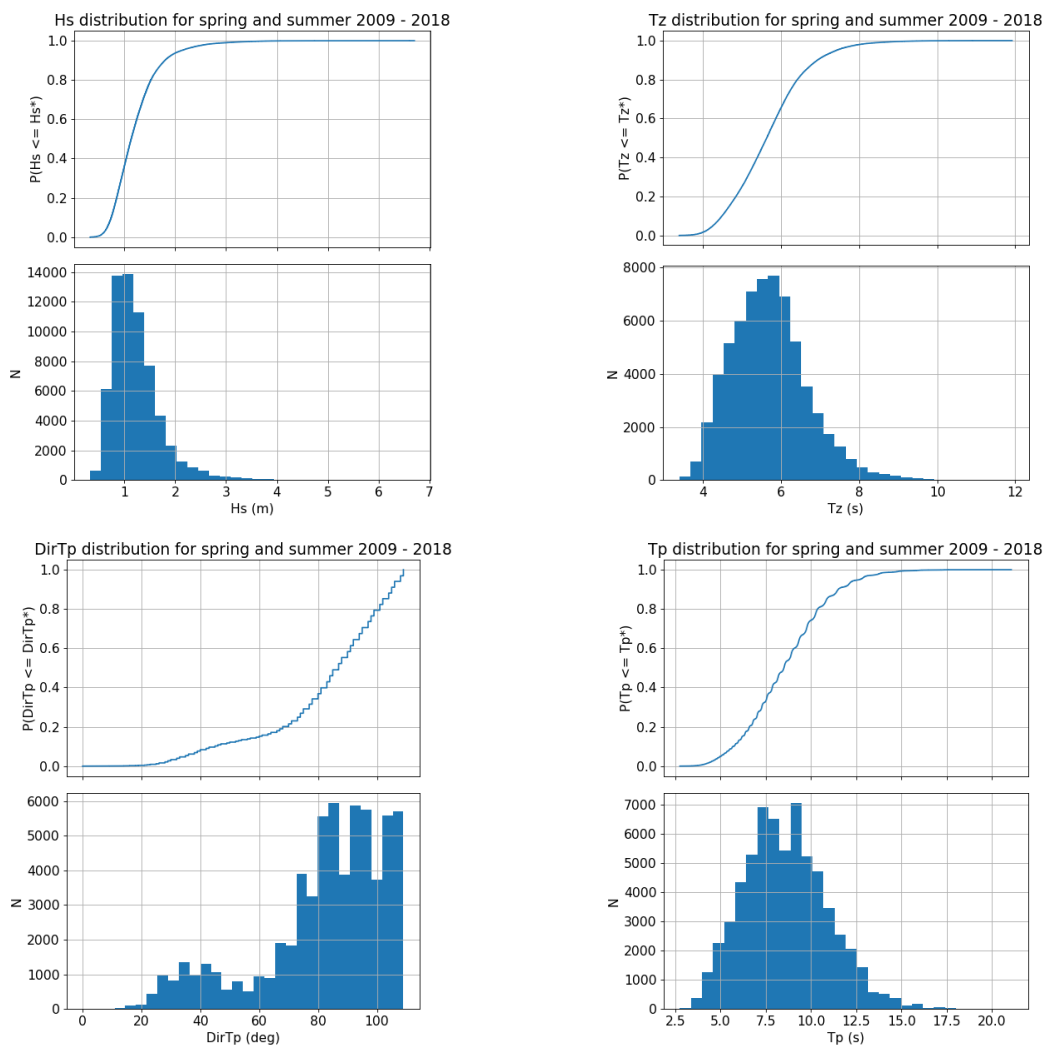
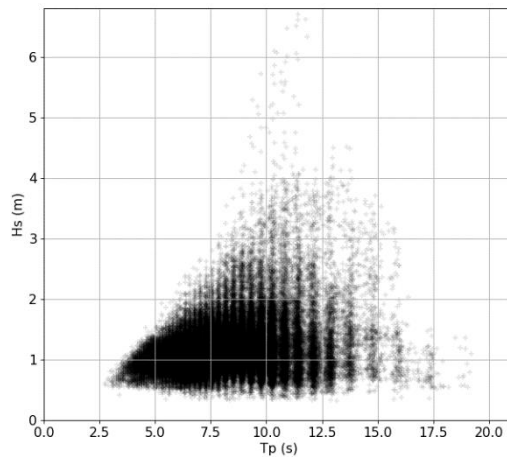


Figure 4. Example of cumulative probability distributions and histograms for long-term spring and summer (September – February) observed data for the Tweed buoy. Data range from 2009 to 2018. Significant wave heights  $H_s$ , zero-crossing period  $T_z$ , peak period direction  $DirT_p$ , and peak period  $T_p$ .



**Figure 5. Scatter plot of significant wave height  $H_s$ , versus peak period  $T_p$  for the 2008 to 2018 monitoring period. Note: the vertical banding present in the higher periods is due to the frequency resolution applied during the spectral analysis.**

### 2.1.1 SWAN

As the deposition location is located between Bilinga and Tugun (see Figure 3), which is approximately 8km (NW) from the Tweed Waverider buoy, a local SWAN model (Peach 2020) was established to capture wave data at the deposition site. To determine the accuracy of the SWAN model, the Tweed and Brisbane buoy data were compared to the SWAN model's results (Figure 6). While Figure 6 demonstrates a reasonable correlation between the model and observed data, it is evident that the model's outputs tend to slightly underestimate wave height. This underperformance can be attributed to the wave energy input from the CAWR wave Hindcast (Durrant 2014) into the SWAN model domain. The CAWCR hindcast already shows a lower  $H_s$  suggesting lower energy into the model.

To gain a better understanding of the local wave climate at the deposition site and to compare the local wave conditions to the Tweed buoy, the SWAN model was run for the last two years, from September 2018 to September 2020, and wave data was extracted from the vicinity of the potential deposition site (see Figure 3).

Based on the SWAN model results (Figure 7) and wave data from Tweed buoy (Figure 4), a range of wave heights and periods were identified. A few indicative conditions were selected to be run at two water levels corresponding to mean sea level (MSL) and lowest astronomical tide (LAT) (Table 1). These wave conditions are selected based on the objectives of the project: To investigate wave breaking for a range of conditions across various dredge deposition mound shapes to assist in the calibration and validation of the numerical model, SWASH. The wave conditions were selected taking into consideration the restrictions on mound placement depth. Since the mound has a crest depth of 4-5 m, it is not anticipated that smaller, more common wave conditions will be significantly affected by the mound; thus, they were not selected. Regular waves are employed to conduct sensitivity tests on the structure to determine the presence and type of wave-breaking under various steepness wave heights and depths in order to calibrate SWASH.

**Table 1. Prototype-scale regular and irregular wave height and period combinations.**

Regular waves		Irregular waves	
$H$ (m)	$T$ (s)	$H_s$ (m)	$T_p$ (s)
0.8	7	1.1	9.2
1	10	1.8	11.5
1.2	9	3.5	11
1.8	11		
3	13		

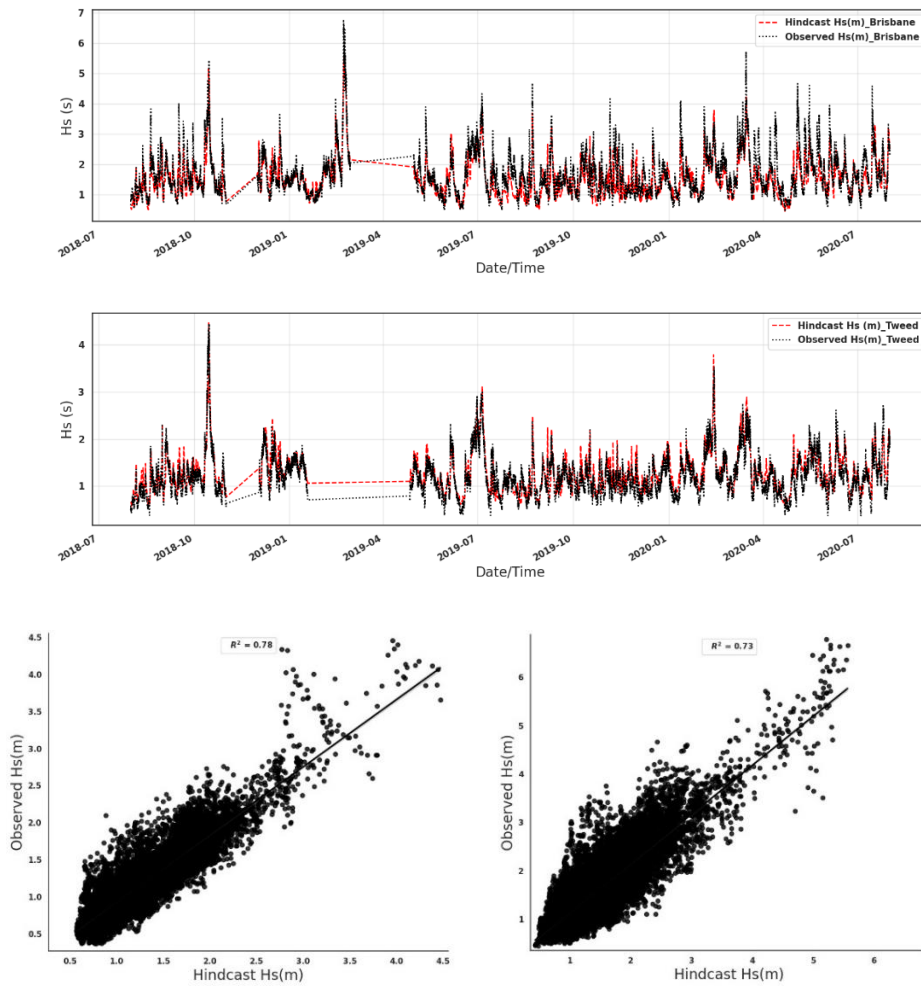


Figure 6. (top) A timeseries plot of the observed  $H_s$  and SWAN results for Brisbane and Tweed. (below) A scatter plot and  $R^2$  values depicting a comparison between the observed  $H_s$  and SWAN results for Brisbane (Right picture) and Tweed (left picture).

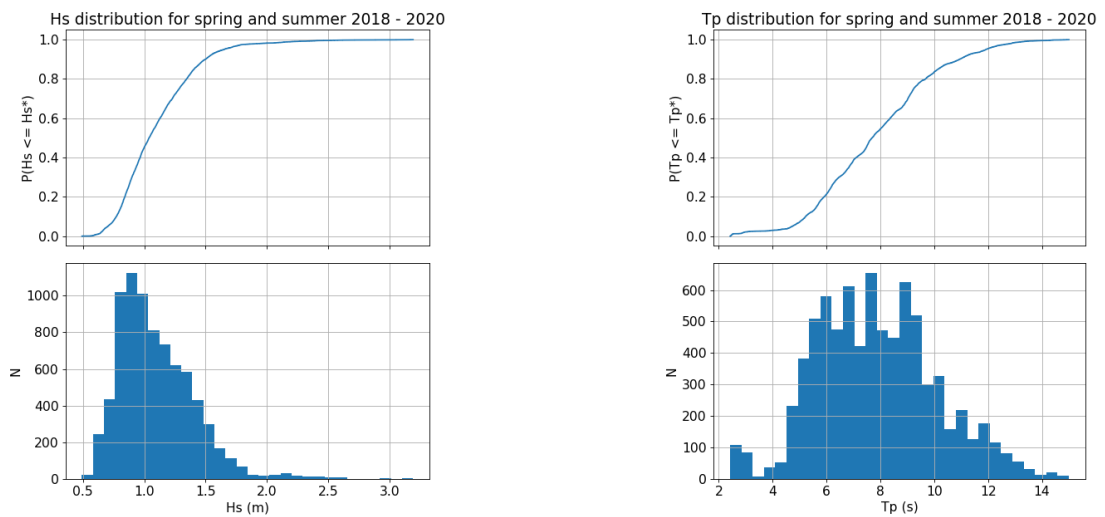


Figure 7. Histograms for spring and summer (September – February) SWAN model data for the area close to the deposition site. Data range from 2018 to 2020. Significant wave heights  $H_s$  and peak period  $T_p$ .

2.2 Initial placement design investigation using Mike21SW

In the first stage of numerical modelling, to gain a better understanding of the required shape, orientation and location of the mound, a simple spectral wave model, Mike21SW, was developed. Being a spectral wave model that solves the spectral action balance equation, its accuracy in areas of shallower water is limited. However, due to its low computational cost for running the model, it was utilized to provide some preliminary results and exclude some unsuitable deposition shapes.

A flexible unstructured mesh was employed to build the model, providing coarser spatial resolution in the offshore area and finer resolution in the area of interest close to the sand mound (Figure 8). ETA 22 profile was used for creating a simple cross-shore profile that was uniform in the longshore. After testing several mound shapes in various water depths, a final shape and location of the mound was selected as shown in (Figure 9). As an example, the results of Mike21 SW model for this mound are shown in Figure 10 which indicates breaking waves at least in low water level condition.

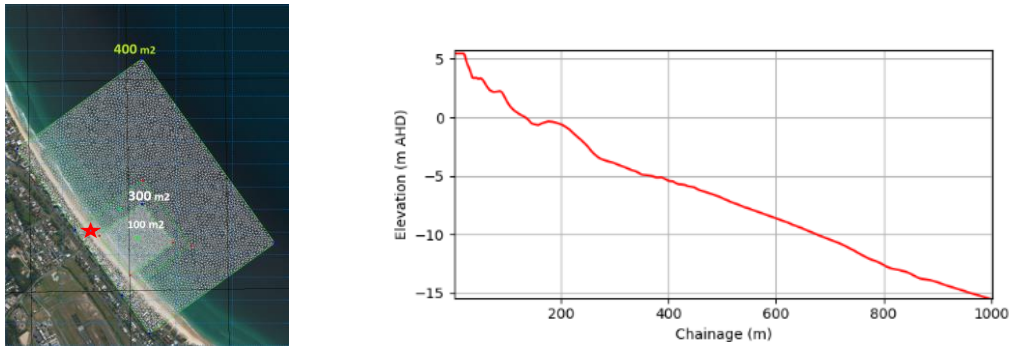


Figure 8. (left) Unstructured mesh with different resolution from offshore (max area limited to 400 m<sup>2</sup>) to near the mound area (Max area limited to 100 m<sup>2</sup>). A red star indicates the approximate beginning point of the ETA 22 profile. (right) ETA 22 profile for building a cross-shore uniform profile.



Figure 9. Final design of the sand mound to be tested further in the QGHL lab.

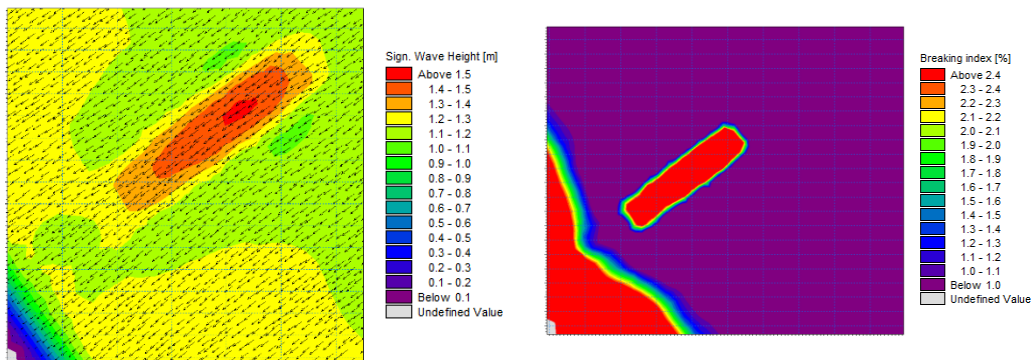
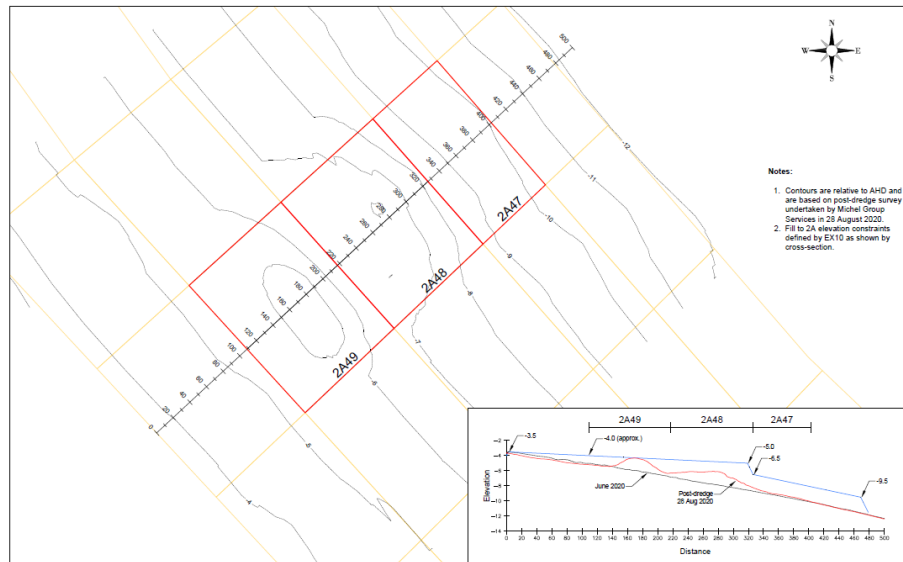


Figure 10. Mike21SW results for the initial mound. (left) significant wave height and direction. (right) showing potential wave breaking over the mound for the low tide condition with  $WL= LAT$ ,  $Hm0= 1.1m$ ,  $Tp= 10s$ .

### First Sand mound design

During the August 2020 dredging campaign, 30,000 m<sup>3</sup> of sand was available to attempt a target placement before any modelling had occurred. The target shape was determined considering the placement depth limitations of the dredge through bottom dumping. The minimum water depth for bottom dumping of the fully laden dredge vessel is five metres. Therefore, a mound shape was selected that was anticipated to have a focusing-effect on the waves to potentially improve breaking characteristics in the lee of the mound. Figure 9 shows the target shape of the sand mound, and Figure 11 shows the final placed mound shape at the field site.



**Figure 11. The main image provides a contour plot showing the final shape of the Bilinga mound. The inset image provides the cross-shore centre-line elevation profile with placement limits indicated by the blue line.**

The final placed mound did not match the intended design and featured two distinct crests along the centre-line profile (Figure 11) instead of the intended longer, straighter, and shallower crest. The final crest elevation along the centre-line profile aligned with the placement limit at the landward extent mound for approximately 20 m before sloping downwards and deviating from the target profile. The mound placement was a relatively last-minute opportunity. With the other beaches determined to be in a healthy state a fortnight before the dredging commenced, only one week was available to decide on the targeted placement design. Therefore, the lack of conformance to the target shape is thought to be partly due to the limited time available to refine the design of the mound and identify an achievable placement methodology in discussion with the dredge operator.

The primary purpose of the dredge depositions is to nourish the Gold Coast beaches. Therefore, the Bilinga mound was not expected or intended to remain forever. However, the mound remained visible as a coherent feature (Figure 12, left), influencing the nearshore wave climate, until two significant storm events in December 2020 and January 2021. The storms produced a large bar that engulfed the mound (Figure 12, right), thereby integrating the deposition into the nearshore active profile and completing the primary purpose of nourishing the beach profile. While the mound did not conform to the target shape, anecdotal reports have indicated that surfers enjoyed relatively consistent, surfable waves in the lee of the mound while it remained as a coherent feature. Unfortunately, there was no formal data collected following this placement to confirm the reports.



**Figure 12. Mound is visible approximately eight weeks after placement (left) and subsequently engulfed by the storm bar (right) following the December and January storms. Yellow circles assist in showing the approximate mound location for comparison of the two images.**

## 2.3 Physical and numerical modelling

### 2.3.1 Physical and numerical modelling setup

A series of physical model tests were conducted at QGHL wave basin in order to:

- Assess the potential of targeting dredge depositions to improve surf amenity.
- Provide benchmark data for validating the SWASH model.

#### *Bathymetry and sand mound*

It was important to produce a representative bathymetry that would allow representative wave transformation over the model domain on the approach to the structure and in the lee of it, with a beach to allow the waves to runup naturally. The TSB dredge campaign typically takes place between July and September when required. Figure 13 shows the measured nearshore profiles at this time of year, which demonstrate reasonable repeatability (excepting the one storm bar present in 2019, and diminishing offshore deposit below  $-5$  m AHD). These profiles indicated that a simplified bathymetry featuring representative planar slopes would suit the model (Figure 13). Comparing the neighbouring survey lines (ETA21 and ETA23, not shown) indicated that the bathymetry at the field site is reasonably alongshore-uniform. Therefore, the model bathymetry was also represented by a simplified alongshore-uniform bathymetry featuring representative planar slopes.

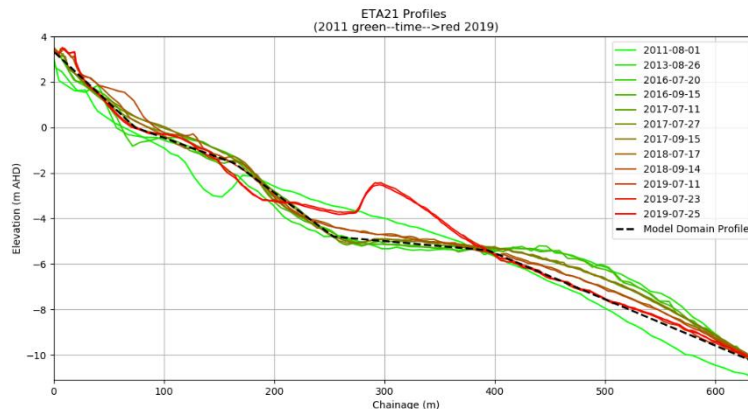


**Figure 13. Nearshore bathymetry measured between July and September for the period 2011 (green) to 2019 (red). Dashed black line is the idealised profile to be used in the physical model.**

The model bathymetry was a fixed concrete bed, and its construction was a multi-stage process. A compacted road base fill (compacted in layers of  $\sim 300$  mm) was introduced to ensure a stable base (Figure 14). Next, concrete (20 MPa, 10 mm aggregate) was poured and screeded to follow surveyed benchmark pins with a thickness of approximately 70 mm (Figure 14).



**Figure 14. Basin bathymetry construction- left, road base fill progressing. Middle, road base fill and elevation check. Right, Concrete pour progressing.**

The first model mound in the lab was built to closely represent the Bilinga mound in 2020. The core of the mound was comprised of compacted sand, placed to develop the shape of the structure onto which a ~20 mm thick concrete cap was placed on top to achieve the target elevations. The final mound was laser scanned and indicative contour lines were painted onto the surface (Figure 15).



**Figure 15. Completed mound with blue and white alternating contour lines indicating elevations corresponding to -5 (small blue crest line, right side of image), -6, -7, -8, -9, and -10 (far left white line) m AHD.**

#### *Numerical modelling*

The non-hydrostatic wave-flow model SWASH was used to model wave transformation and breaking in nearshore areas (Zijlema 2011). SWASH is a phase-resolving model that solves non-linear shallow water equations including a non-hydrostatic pressure term. SWASH can account for wave propagation, frequency dispersion, shoaling, refraction, diffraction, wave breaking and nonlinear wave-wave interactions. These physical processes are essential for modelling surf amenity conditions. Applying a phase resolving model allows simulating the details of wave crest patterns as waves propagate towards the surf zone, and identifying possible wave focusing which may enhance surfing conditions. Simulation of surf zone dynamics, including wave-driven current and wave breaking patterns, creates a better picture of overall wave breaking footprints as well as key elements of the surf break circulation (Weppe 2019).

The numerical domain in SWASH was created using 1020\*470 grid cells, with a spatial resolution of 0.03125m (corresponding to 1m x 1m at the prototype scale, Figure 16). The numerical model bathymetry was the same as physical model bathymetry, which had been extracted using a Leica MS60 laser scanner with a resolution of 10mm. To avoid applying a high number of vertical layers, wave breaking was taken into account using the hydrostatic front approximation (SWASH team 2021). Following Zijlema (2011), the discrete upwind momentum-conservative advection scheme was used for running SWASH. The initial time step was set to 0.005 seconds, and automatically adjusted during the calculation to maintain a maximum CFL (Courant–Friedrichs–Lewy) number of 0.5. The numerical model was set to run for a duration of 55 seconds, with 10 seconds for both the wave ramp up and ramp down. This time frame was the same as that used for the physical model simulations. The wave boundary conditions (only regular waves) used in the numerical model runs were identical to those of the physical modelling as shown in Table 1. The time series of the wave record at wave generator paddles was prescribed as the wave boundary condition of the numerical model.

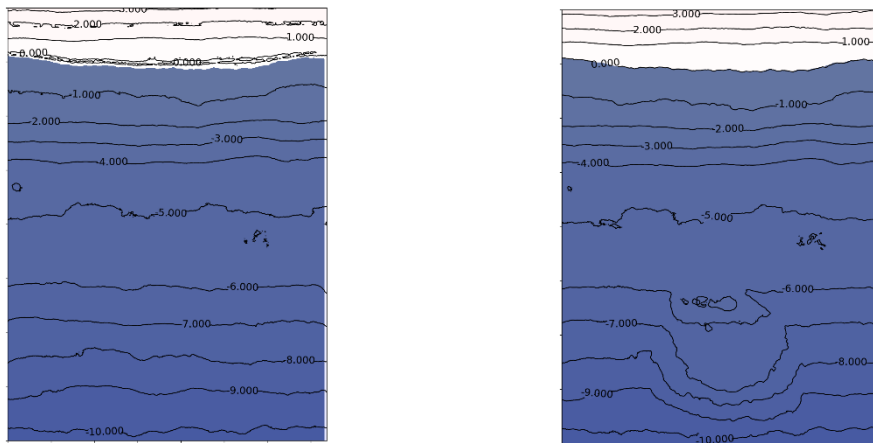


Figure 16. Water depth (MSL) and model domain dimension for base condition – no mound (left) and mound 1 (right).

### 3. Results

This section presents the results of the physical and numerical model testing undertaken as part of the investigation into the use of targeted sand placements to enhance surf amenity. The results of the baseline tests (without mounds) and mound#1 are presented in section 3.1, followed by the results of the second mound configurations in section 3.2. The section 3.3 concludes with a discussion of future steps.

#### 3.1 Baseline (no mound) and mound #1 tests (TS1)

##### *Physical modelling*

Test Series 1 (TS1) was used as a baseline to capture and observe wave transformation data as the waves propagated over the model bathymetry with no mound. The longshore-uniform bathymetry resulted in reasonably longshore uniform wave transformation and breaking in the model (top photos, Figure 17). Therefore, for expediency, the wave measurements for this test series only occurred along the centre line. The regular and random wave test conditions (i.e. conditions at the wave paddle) are detailed in Table 1.

Test Series 2 (TS2) was the first test series that featured a mound, which closely represented the field site placement during the 2020 TSB dredging campaign (Figure 15). The mound introduced variability on the underlying alongshore-uniform seabed profile, influencing wave transformation processes. As can be seen from Figure 17, of the two regular wave conditions tested, the larger ( $H = 3$  m,  $T = 13$  s) broke over the seaward slope of the mound, approximately following the  $-7$  m AHD contour. The waves for the smaller condition ( $H = 1.8$  m,  $T = 11$  s) broke in the lee of the mound, exhibiting a focusing effect where the waves broke first in deeper water in the centre of the basin at a depth of approximately five metres (Figure 17). The non-focused regions of the wave crests (away from the centre, toward the basin walls) broke closer to the  $-3.5$  m AHD contour, which is a comparable depth to the TS1 case with the same conditions. The CH06 probe (Figure 18) measured the largest average wave height in the focused region along the centre line with a prototype  $H_{ave} \approx 3.5$  m, almost double the wave height at the paddle.





Figure 17. The top photos depict the wavefield in the baseline, no-mound conditions during TS1. With no mound, the waves can be seen to be breaking relatively uniformly in the longshore. The bottom photos show the wavefield with the first mound in place. The presence of the mound resulted in more variability in the breakpoints with the larger waves breaking over the mound (lower left image) and smaller waves breaking in the lee of the mound, demonstrating the focussing effect.

Figure 18 provides two contour plots of the model domain average wave heights ( $H_{ave}$ ) for the regular wave conditions at  $WL = 0$  m AHD. The contour data have been linearly interpolated from the 43 wave probe locations (grey dots in each plot). These plots demonstrate the variability in the nearshore wave transformations due to the mound, and the highest contours indicate the approximate breakpoint locations.

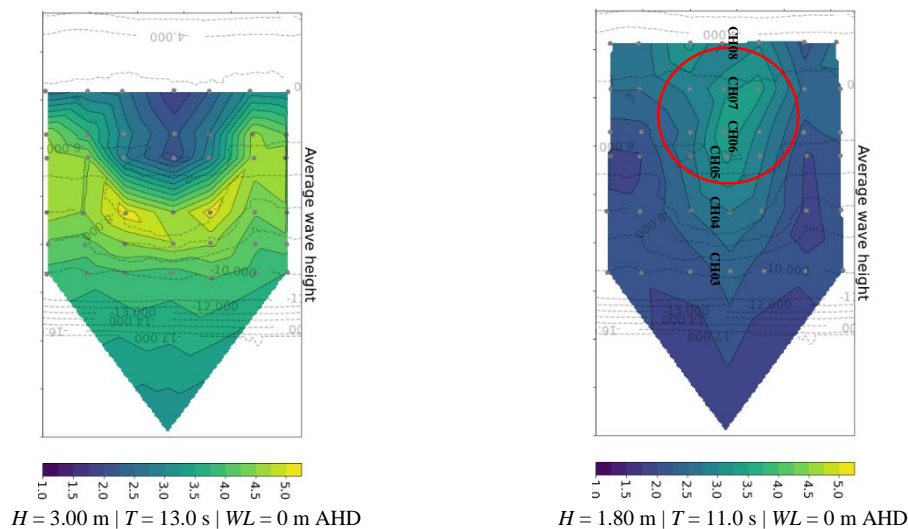


Figure 18. Average wave height plots for the regular wave conditions detailed below each plot. Waves propagate shoreward from bottom to top. The red circle highlights the wave focussing region in the lee of the mound for the smaller wave case. The contour data are interpolated between each probe location (grey dots). The black labels along the centre line probes in the right plot indicate the probe (CH0#) order for each cross-shore transect.

#### Numerical modelling

The results from the initial physical model tests for the first mound were utilized to calibrate and validate the SWASH model. To compare the breaking patterns observed in the physical model and SWASH, the largest regular wave condition was employed. To identify breakpoints, Python was used to detect wave pockets, plotting black dots for left-hand waves and white for right-hand waves (Figure 19).

As seen in the illustrations in Figure 19, the break points in the physical model followed the -7m contour, resulting in a U-shaped breaking pattern. However, the SWASH model did not produce the same pattern as seen in the left image of Figure 19. The inadequate performance can be attributed to the embedded assumptions of the SWASH model, which was designed for mild shoreline slopes rather than rapidly changing bathymetry like reef slopes. To gain insight into why the breaking patterns differ between SWASH and the physical model, further research was conducted into how wave breaking is simulated in SWASH.

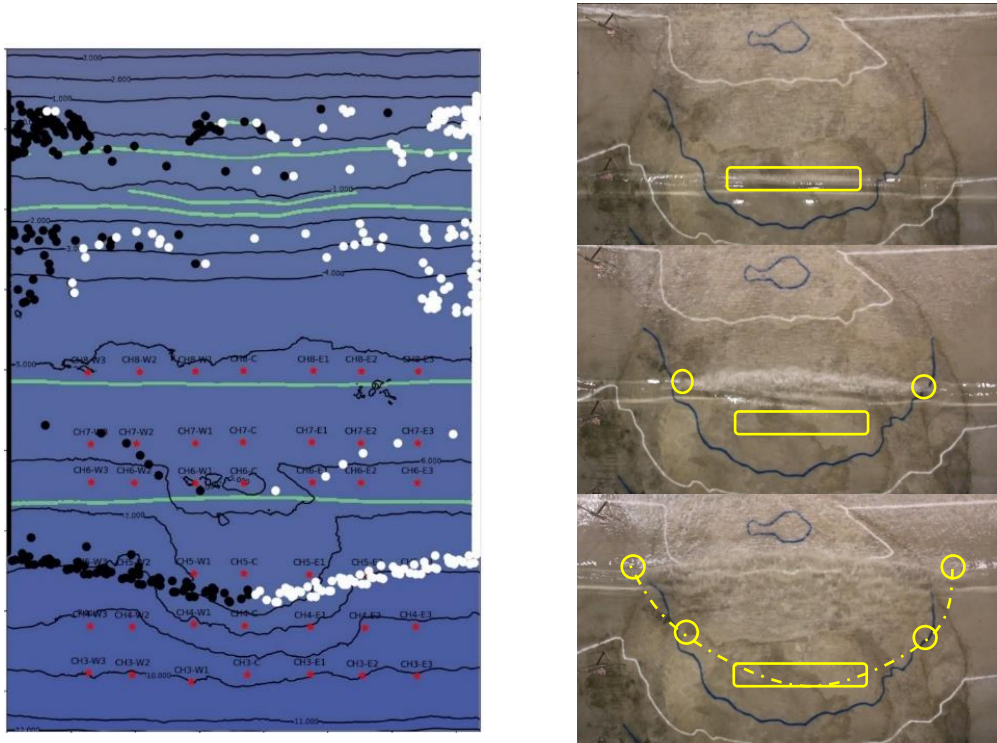


Figure 19. The breaking results of SWASH and physical models for regular waves with  $H = 3.0$  m |  $T = 9.0$  s |  $WL = 0$  m AHD.

In SWASH wave breaking is initiated when the vertical speed of the free surface exceeds a fraction of the shallow water celerity, as follows (SWASH team 2021):

$$\frac{\partial \eta}{\partial t} > \alpha \sqrt{gh} \quad [1]$$

Where  $\eta$  is water level,  $t$  is time,  $\alpha$  is threshold parameter at which to initiate wave breaking,  $g$  is the gravitational acceleration, and  $h$  is water depth.

The “breaking parameter”  $\alpha > 0$  represents the maximum local surface steepness and determines the onset of the breaking process. SWASH applies a default threshold value of  $\alpha = 0.6$ . To represent persistence of wave breaking, SWASH also labels a grid point for hydrostatic computation (breaking) if a neighboring grid point has been labelled for hydrostatic computation and the local steepness is still high enough, i.e.,

$$\frac{\partial \eta}{\partial t} > \beta \sqrt{gh} \quad [2]$$

Where the “persistence parameter”,  $\beta$  is threshold parameter (default value,  $\beta = 0.3$ ) which determines the extent of wave breaking beyond the cells identified as breaking through Eq. [1].

Considering the fact that  $\frac{\partial \eta}{\partial t}$  is kinematically related to the slope of the free surface  $\frac{\partial \eta}{\partial x}$  for a progressive wave, lower values of  $\alpha$  decreases the threshold surface slope for the onset of wave-breaking, thus allowing for less steep wave faces prior to wave-breaking and moving the break point seaward (Buckley 2014). Similarly decreasing  $\beta$  values moves the breakpoint seaward.

The default breaker ( $\alpha$ ) and persistence ( $\beta$ ) parameters in SWASH resulted in a different pattern of breaking compared to the physical modeling. Adjusting the two parameters to  $\alpha=0.55$ ,  $\beta=0.4$  resulted in a breaking pattern that better aligned with that observed in the physical model (Figure 20). The newly calibrated SWASH model was also tested against the smaller wave condition ( $H = 1.8$  m,  $T = 11$  s) to compare the characteristics of the breaking zone (Figure 21).

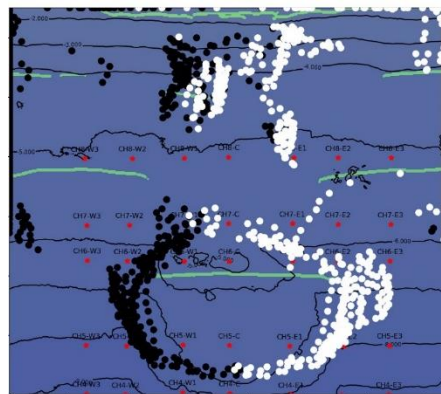


Figure 20. Breaking pattr in the calibrated SWASH.  $H = 3.0\text{ m}$  |  $T = 13.0\text{ s}$  |  $WL = 0\text{ m AHD}$ .

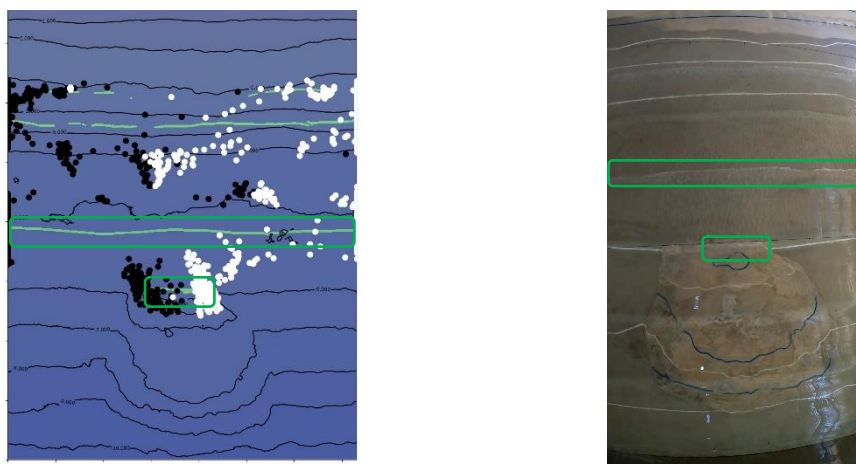


Figure 21. The breaking results of SWASH and physical models for regular waves with  $H = 1.8\text{ m}$  |  $T = 11.0\text{ s}$  |  $WL = 0\text{ m AHD}$ . Green boxes on the right image indicate the start of wave breaking and a fully broken wave crest in the physical model, which is comparable to the highlighted broken wave crest in the left image.

In addition to the analyses of the breaking patterns, the calibrated SWASH model was utilised to estimate the water surface elevations at the same point locations used in the physical model tests. Similar to Figure 18, average wave heights were then plotted from the SWASH results, as seen in Figure 22. There are evidently disparities between physical modelling and SWASH results, yet one can also observe that SWASH is effectively capturing the contours of the wave height distributions.

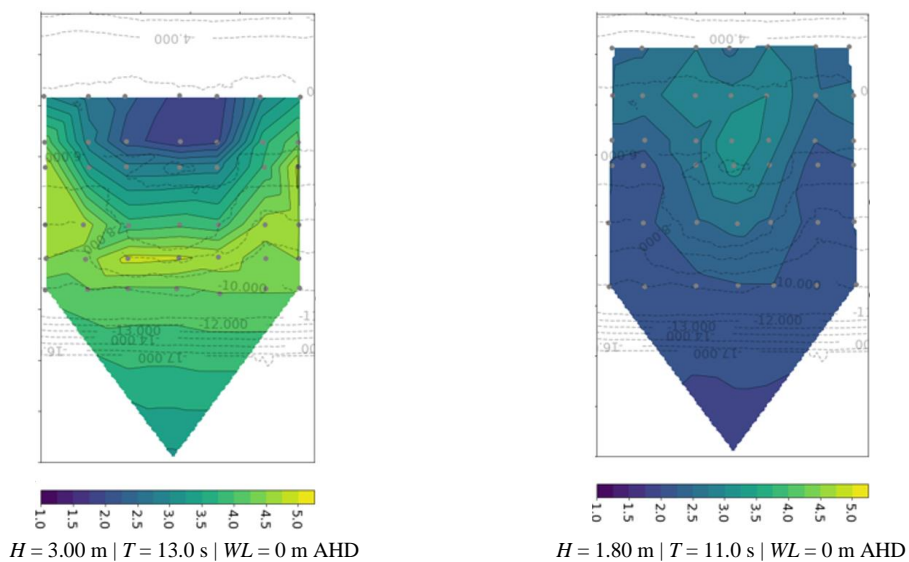


Figure 22. SWASH average wave height plots for the regular wave conditions.

### 3.2 Mound #2 tests (TS2)

Using the calibrated SWASH model, the next mound was designed using SWASH featuring a shallower crest depth of  $-3\text{m AHD}$ , an asymmetrical shape, and a longer crest at a  $45\text{-degree}$  orientation, intended to produce a right-hand breaking wave. This mound generated wave-breaking over the crest for all conditions tested, with a single, 'right-hand' breakpoint direction (approaching the shore).

Figure 23 shows that the white-dot breakpoint trajectory follows the crest in the right image, similar to the breakpoint tracks seen in the physical model (green line on the left image). Considering the different orientation, depth, dimension and slope between the first and second mounds, and given the satisfactory prediction of breakpoints in SWASH, this was considered to demonstrate a reasonable validation of the calibration applied during TS1. Therefore, pending further validation on a prototype scale, the calibrated SWASH model has potential for use as a design tool for the placement of artificial sand mounds.

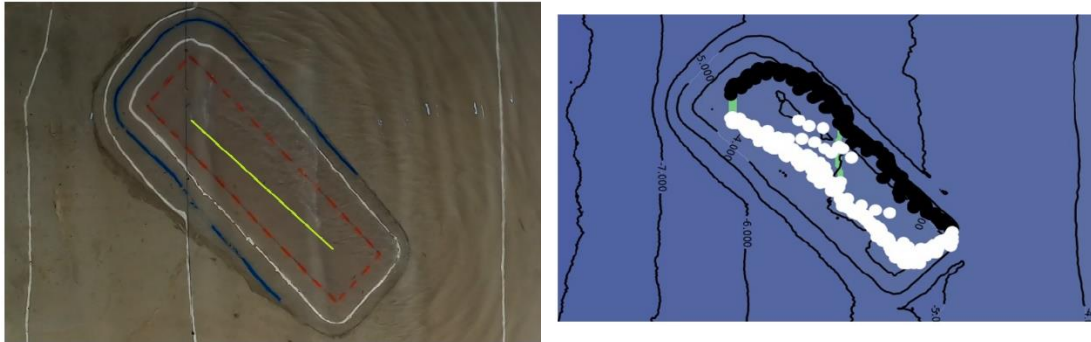


Figure 23. The green line (left) and white dots (right) indicate the breakpoint tracks in the physical and numerical models for the second mound design. Waves propagate from left to right.  $H = 1.2\text{ m}$  |  $T = 13.0\text{ s}$  |  $WL = 0\text{ m AHD}$ .

Figure 24 provides a comparison of the wave field in the numerical and physical models, with red lines highlighting some of the features. It can be seen that SWASH has reasonably captured the shape of the wave crests over and in the lee of the mound, including higher harmonics after breaking and ripples.

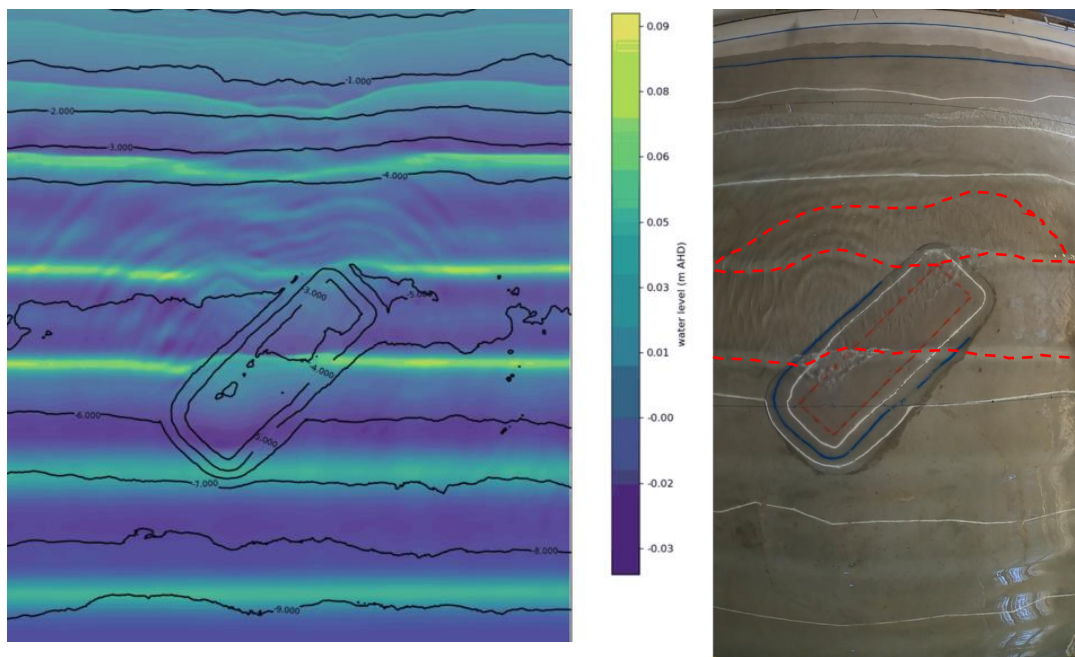


Figure 24. A comparison of the wave field in the numerical and physical model, with red lines highlighting some of the features.

### 3.3 Next steps

To validate SWASH in the prototype scale, the next mound has been designed using the calibrated SWASH model, which has also been built and tested in the physical model. This mound is intended to be placed during the dredge campaign in 2023. To increase the likelihood of success, a dredge operator was involved in the discussions during the design process of this mound to devise a design that allowed for a workable placement strategy. The design features side slopes close to the anticipated natural sand settling slope when bottom dumped. To compare the field data with the outputs of the calibrated SWASH model, a data collection campaign is also intended at the field site to collect video, pressure transducer, and wave buoy data just offshore at the site.

### 4. Conclusion

In this paper, the feasibility of using dredge material to improve surf amenity was investigated through physical and numerical modeling. Physical model data was used to test deposition mound designs in order to initially calibrate and validate a numerical model, SWASH. It was found that SWASH generally reproduced the wave height over and in the lee of the mound with reasonable accuracy. However, tuning of the breaking parameters ( $\alpha$  and  $\beta$ ) was necessary to accurately simulate the onset and persistence of the breaking process. The calibrated SWASH model proved to be a useful tool for gaining a better understanding of key features of nearshore wave propagation and wave breaking.

Larger waves broke in two directions over the first mound, and smaller waves reacted to the mound, changing direction, exhibiting a focusing effect that generated wave breaking in the deeper water in the lee of the mound. The shallower, obliquely-oriented second mound generated wave-breaking along the crest for all conditions tested, with a single, 'right-hand' breakpoint direction (approaching the shore). SWASH breakpoints trajectories were close to those observed in the physical model (Figure 23).

These preliminary physical and numerical modeling results indicate potential surf amenity benefits in engineering design of dredge placement. Additionally, to further ensure the accuracy of SWASH at the prototype scale, a successful field placement of the modelled mound needs to be achieved in order to compare the results with the reduced-scale physical and numerical models.

### ACKNOWLEDGMENTS

The authors wish to express their gratitude to several parties. Firstly, the TSB team is recognized as a crucial stakeholder for funding the project and their continued involvement in this investigation. Additionally, the authors extend their appreciation to the Queensland Government Hydraulics Laboratory for supplying wave data and assisting with multiple physical modeling tasks. Lastly, the City of Gold Coast is acknowledged for providing beach profile data for the site.

### REFERENCES

- Booij N, Ris RC, Holthuijsen LH. A third-generation wave model for coastal regions 1. model description and validation. *J Geophys Res.* 1999; 104(C4): 7649- 7666.
- Buckley, M., Lowe, R. & Hansen, J. Evaluation of nearshore wave models in steep reef environments. *Ocean Dynamics* 64, 847–862 (2014). <https://doi.org/10.1007/s10236-014-0713-x>
- Colleter, G., Parnell, K., Wharton, C., & Hunt, S. (2019, January). Beach nourishment pattern-placement along the Gold Coast. In *Australasian Coasts and Ports 2019 Conference: Future directions from 40 [degrees] S and beyond*, Hobart, 10-13 September 2019 (pp. 206-212). Hobart: Engineers Australia.
- Durrant, T., Greenslade, D., Hemer, M., Trenham, C., 2014. A Global Wave Hindcast focussed on the Central and South Pacific. CAWCR Technical Report 070 This will open in a new window.
- Peach, L., Carthwright, N., & Strauss, D. (2020). INVESTIGATING MACHINE LEARNING FOR VIRTUAL WAVE MONITORING. *Coastal Engineering Proceedings*, (36v), papers.46. <https://doi.org/10.9753/icce.v36v.papers.46>
- Raybould, M., Anning, D. (2020). Economic and Social Impacts of the Tweed Sand Bypass (TSB). NSW Department of Planning, Industry, and Environment.
- SWASH team, 2021. SWASH user manual version 7.01. <http://www.tudelft.nl/swash>
- Weppe and Shand, 2019. Modelling surf break wave mechanics with SWASH - an application to Mangamaunu Point Break (Kaikōura, New Zealand)
- Zijlema, M., Stelling, G. and Smit, P., 2011. SWASH: An operational public domain code for simulating wave fields and rapidly varied flows in coastal waters. *Coast. Engng.*, 58, 992-1012.
- Zijlema, M., Stelling, G., & Smit, P. (2011). SWASH: An operational public domain code for simulating wave fields and rapidly varied flows in coastal waters. *Coastal Engineering*, 58(10), 992-1012. doi: 10.1016/j.coastaleng.2011.05.015